Supporting Information for

Thin and flexible Fe–Si–B/Ni–Cu–P metallic glass multilayer composites for efficient electromagnetic interference shielding

Jijun Zhang[a,b,c], Jiawei Li[a,b], Guoguo Tan[a,b], Renchao Hu[a,b], Junqiang Wang[a,b],*

Chuntao Chang[d], Xinmin Wang[a,b]

[a]Key Laboratory of Magnetic Materials and Devices, Ningbo Institute of Materials Technology & Engineering, Chinese Academy of Sciences, Ningbo 315201, China

[b]Zhejiang Province Key Laboratory of Magnetic Materials and Application Technology, Ningbo Institute of Materials Technology & Engineering, Chinese Academy of Sciences, Ningbo 315201, China

[c]University of Chinese Academy of Sciences, Beijing 100049, China

[d]Dongguan University of Technology, Dongguan 523808, China

*Corresponding author

Name: Jiawei Li;
E-mail: lijw@nimte.ac.cn;
Tel: +86-0574-87617212

This PDF file includes:

      Supplementary Text

      Figures S1to S8

      Tables S1 to S3

Electrical Conductivity Measurements

Electrical conductivity of all samples was examined by a standard four-probe method on a Napson Cresbox Measurement System. The four probes were placed at 16 positions one after another of each samples and sheet resistance was recorded. Electrical conductivity of the samples can be figured out by the following equation:

$$\sigma = \left(\frac{1}{R_s t}\right) \tag{1}$$

Where σ is the electrical conductivity [S m^{-1}], R_s is the sheet resistance [Ω sq^{-1}] and t is the thickness of samples [m].

Electromagnetic Interference (EMI) Shielding Measurements

Propagation of electromagnetic waves (EMWs) through a flat composite material characterized by permittivity (ε), permeability (μ) and the thickness (t) is described via a formalism related to electric (E) and magnetic (H) field components. The surface impedance of the flat composite is expressed in matrix form and deduced from the interfaces: imposing electric and magnetic fields on input and output flat shield yields a matrix formulation:[1]

$$\begin{bmatrix} E_{in} \\ H_{in} \end{bmatrix} = \boldsymbol{\Phi} \begin{bmatrix} E_{out} \\ H_{out} \end{bmatrix} \tag{2}$$

Where E_{in}, H_{in}, E_{out} and H_{out} are the electric and magnetic fields on input and output interfaces, $\boldsymbol{\Phi}$ is the transferring matrix of the flat shield.

The EMI shielding effectiveness (SE), is a measure of material's capability to screen EMWs. For a three-layer material, the SE can be expressed in the following form:[2-3]

$$SE = 10 \lg \{0.5[\eta_0^2 \Phi_{21} + \eta_0(\Phi_{11} + \Phi_{22}) + \Phi_{12}]\} \tag{3}$$

Where Φ_{11}, Φ_{12}, Φ_{21}, Φ_{22} are the coefficients associated to of the transferring matrix $\boldsymbol{\Phi}$ of the sheet, and η_0 is the free-space wave impedance.

Experimentally, the total EMI SE (EMI SE_T) is defined as the logarithmic ratio of incident power (P_I) to transmitted power (P_T) of radiation. And SE_T is the sum of the contributions from reflection (SE_R), absorption (SE_A) and multiple reflections (SE_M):[4]

$$SE_T = 10\lg\left(\frac{P_I}{P_T}\right) = 20\lg\frac{1}{|T|} = SE_R + SE_A + SE_M \tag{4}$$

The effective absorbance (A_{eff}), SE_R and SE_A can be calculated as:

$$A_{eff} = \left(\frac{1\text{-}R\text{-}T}{1\text{-}R}\right) \tag{5}$$

$$SE_R = 10\lg\left(\frac{1}{1\text{-}R}\right) = 10\lg\left(\frac{1}{1-|S_{11}|^2}\right) \tag{6}$$

$$SE_A = 10\lg\left(\frac{1}{1\text{-}A_{eff}}\right) = 10\lg\left(\frac{1\text{-}R}{T}\right) = 10\lg\left(\frac{1-|S_{11}|^2}{|S_{21}|^2}\right) \tag{7}$$

In case of higher EMI SE values (>15 dB), SE_M is generally neglected and SE_T can be written as:[5]

$$SE_T \approx SE_R + SE_A \tag{8}$$

The reflection and transmission coefficient are determined by S parameters (S_{11}, S_{22}, S_{12} and S_{21}) measured by the two-port vector network analyzer (VNA). The transmittance (T), reflectance (R), and absorbance (A) through the shielding material can be described as below:[6]

$$R = \left|\frac{E_T^2}{E_I^2}\right| = |S_{11}|^2 = |S_{22}|^2 \tag{9}$$

$$T = \left| \frac{E_R^2}{E_I^2} \right| = |S_{12}|^2 = |S_{21}|^2 \tag{10}$$

$$R + T + A = 1 \tag{11}$$

Where, E_I and E_T are the electric field of incident and transmitted EM waves.

Calculation of skin depth (δ)

The skin depth of a shield, defined as the depth at which electromagnetic energy drops exponentially to 1/e of its incident value, was roughly evaluated according to the following relation:[7]

$$\delta = \frac{1}{\sqrt{\pi f \sigma \mu}} \tag{12}$$

Where δ is the electrical conductivity, f is the frequency and μ is the magnetic permeability.
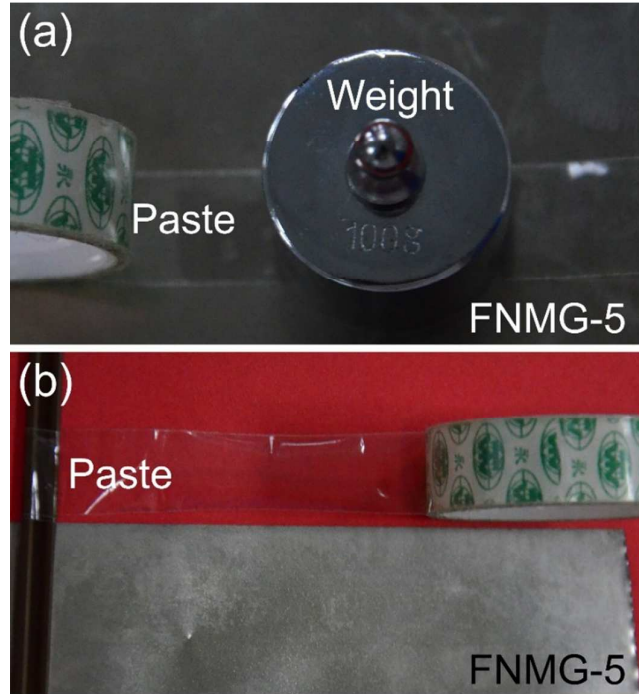

Figure S1. Photographs of the tape test. A scotch tape is pasted on the surface of the FNMG-5 ribbon under a pressure of 1000 N. After stripping the tape away, no

residual Ni–Cu–P coating is seen on the tape, indicating the good bonding strength between Ni–Cu–P coating and Fe–Si–B substrate.
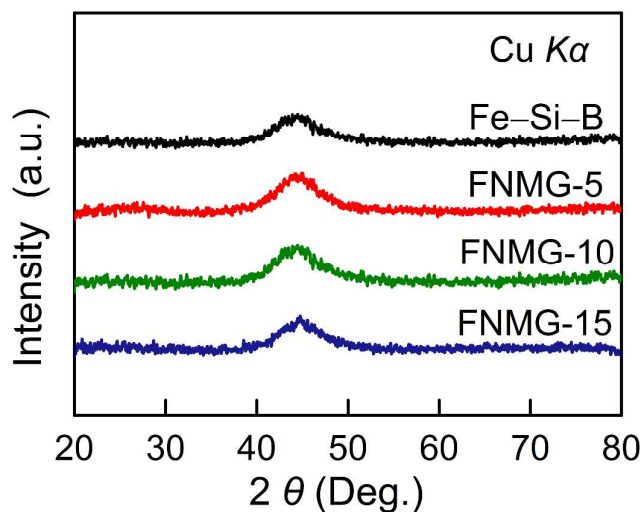

Figure S2. XRD patterns of the Fe–Si–B and FNMG ribbons, indicating the amorphous nature of all FNMG ribbons.
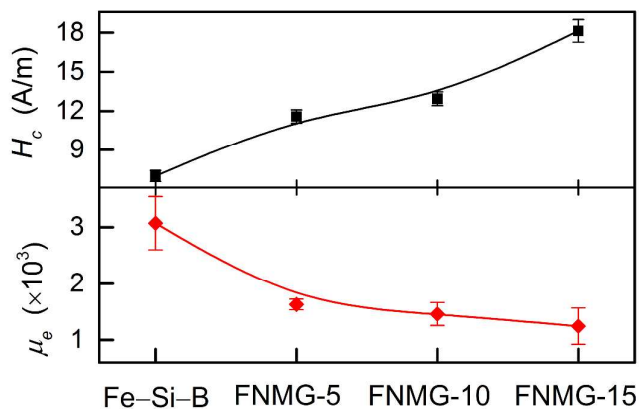

Figure S3. Coercivity and permeability of the Fe–Si–B and FNMG ribbons. The FNMG ribbons possess good soft magnetic properties, showing coercivity less than 20 A/m and initial permeability more than 1000.
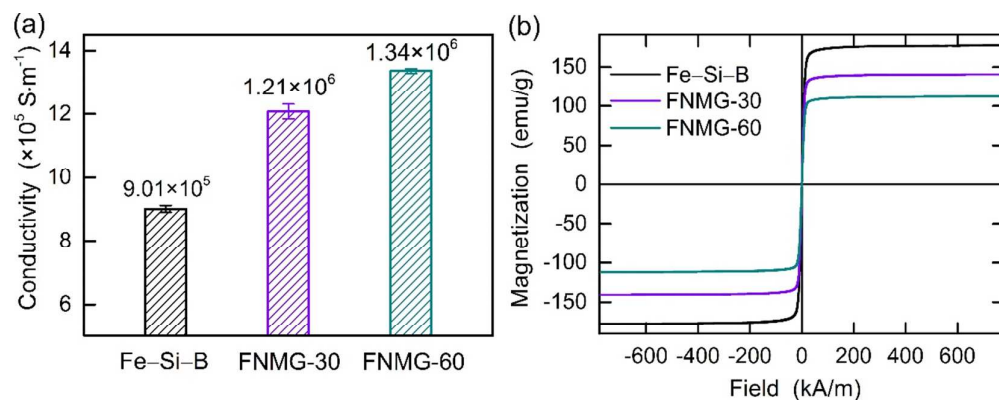
Figure S4. (a) Conductivity plots and (b) VSM curves of the Fe–Si–B, FNMG-30 and FNMG-60 ribbons. Longer deposition time (30 and 60 minutes) induce even bigger increment in conductivity, but at highly cost of soft magnetic properties.
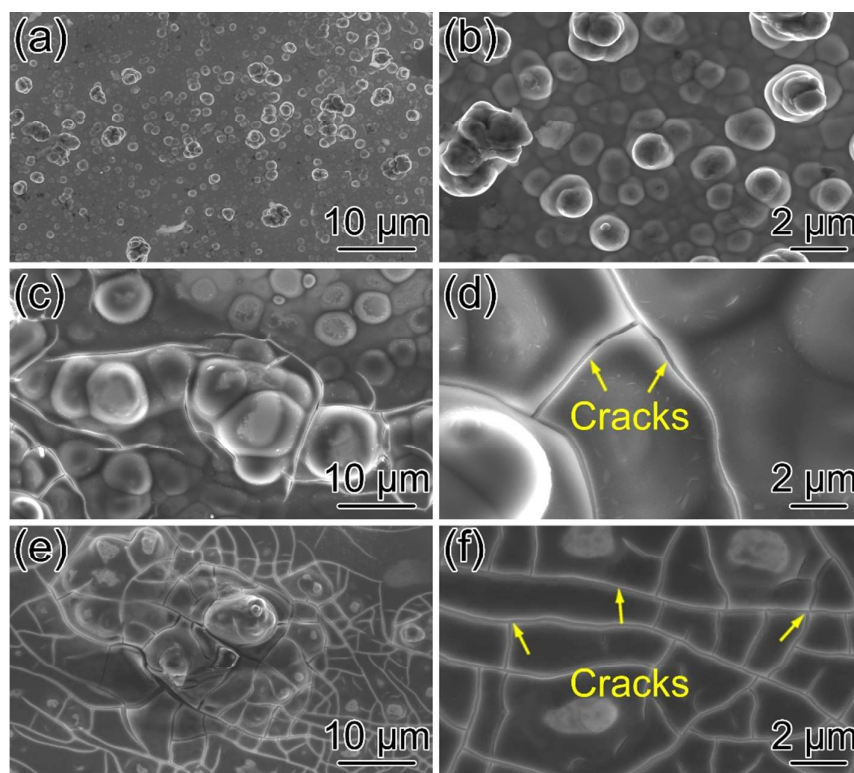

Figure S5. Surface morphologies of the FNMG composite ribbons. (a, b) FNMG-5 ribbon after 100 times bending. No cracks or fissures are presented on the surface of FNMG-5 sample, after 100 times bending. (c, d) and (e, f) As prepared FNMG-30 and

FNMG-60 ribbons. Longer deposition time (30 and 60 minutes) cause cracks in the surface of Ni–Cu–P coating, thus deteriorating flexibility.
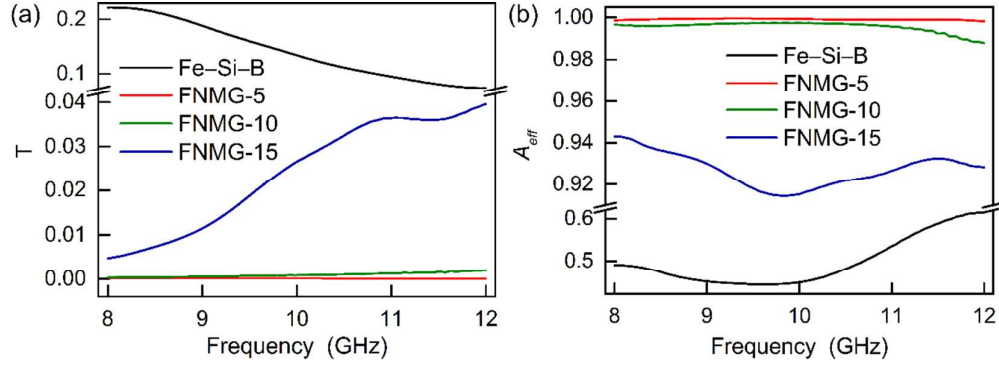

Figure S6. (a) Transmission (T) and (b) effective absorption (A_{eff}) of the Fe–Si–B and FNMG samples. The effective absorption (A_{eff}) at 10 GHz is 0.9999 for FNMG-5 sample, indicating that about 99.99% incident electromagnetic energy has been screened by it.
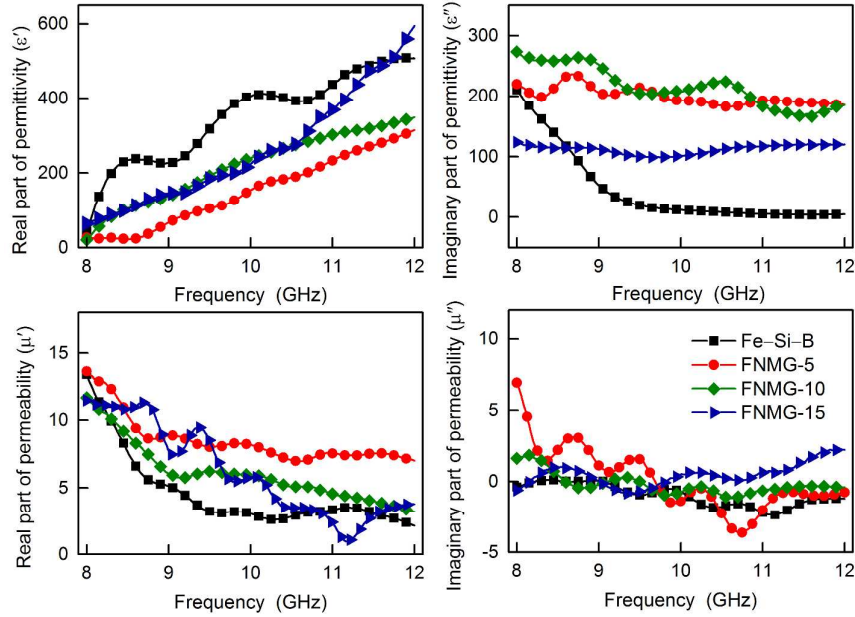

Figure S7. Frequency dependence of (a) the real part (ε') and (b) the imaginary part (ε'') of the complex permittivity, (c) the real part (μ') and (d) the imaginary part (μ'') of the complex permeability of the Fe–Si–B and FNMG samples.
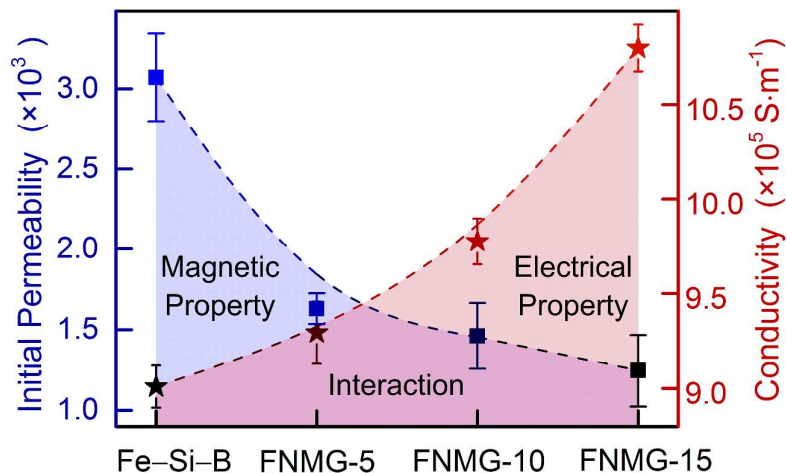
Figure S8. The electroless plating time dependence of initial permeability (left axis) and conductivity (right axis) of the Fe–Si–B and FNMG samples.

Table S1. Chemical composition of the electroless plating bath and operation conditions.

Solution composition	Concentration	Condition
$NiSO_4 \cdot 6H_2O$	20 g/L	
$NaH_2PO_2 \cdot H_2O$	20 g/L	363K
$Na_3C_6H_5O_7 \cdot 2H_2O$	10 g/L	PH : 5~6
$NaC_2H_3O_2 \cdot 3H_2O$	20 g/L	5 minutes
$C_3H_6O_3$	30 g/L	10 minutes
CH_4N_2S	0.003 g/L	15 minutes
$CuSO_4 \cdot 5H_2O$	1 g/L	

Table S2. Summary of electric, magnetic, EMI shielding effectiveness, thermal stability and mechanical performance of FNMG composite. E_{corr}, I_{corr}, R_t and T_x represent the corrosion potential, corrosion current density, charge transfer resistance and crystallization temperature, respectively.

	Fe–Si–B	FNMG-5	FNMG-10	FNMG-15
Conductivity ($\times 10^5$ S/m)	9.01	9.29	9.77	10.80
Initial permeability	3071	1630	1461	1245
Skin depth (1KHz) (mm)	0.303	0.409	0.421	0.434
Skin depth (10GHz) (mm)	0.0030	0.0018	0.0021	0.0020
Coercivity (A/m)	7	11.6	13	18.2
Magnetization (emu/g)	178	172	167	162
EMI SE (8GHz) (dB)	6.6	39.5	35.4	23.5
EMI SE (10GHz) (dB)	8.8	40.9	31.0	15.8
E_{corr} (mV)	-697.4	-558.3	-530.3	-480.4
I_{corr} ($\times 10^{-5}$ A·cm^2)	1.20	1.73	3.06	4.42
R_t (Ohm·cm^2)	457	858	1391	2466
T_x (K)	695	695	696	696
Tensile strength (MPa)	1639	1593	1656	1533

Table S3. EMI shielding performance of various metal based shielding materials.

Filler	Matrix	Thickness	Conductivity	EMI SE	SE/t	Ref.

		[mm]	[S m^{-1}]	[dB]	[dB mm^{-1}]	
Ni	PP	3	100	20	6.7	25
Ni	PVDF	1.95	<0.1	23	11.8	24
Ag/CF	Epoxy	2.5	/	38	15.2	22
Ag Nanowires	PS	0.8	1.9×10^3	33	41.3	23
Cu Nanowires	PS	0.2	/	35	175	20
Al Flakes	PES	2.9	/	39	13.4	21
SS	PP	3.1	0.1	48	15.5	26
SS	PES	3.08	/	35	11.4	21
Fe$_2$O$_3$	PP	2	/	22.8	11.4	19
Fe$_3$O$_4$	PEI	2.5	/	18.2	7.3	15
Cu (T2)	/	0.11	3.8×10^7	10.7	97.3	This work
Cu (T2)	/	1	3.5×10^7	27.4	27.4	This work
Cu (H62)	/	0.95	1.1×10^7	21.8	23.0	This work
Al	/	0.45	1.2×10^7	11.2	24.9	This work
SS	/	1.79	4.5×10^5	23.6	13.2	This work
Si steel	/	0.23	1.6×10^6	13.7	59.6	This work
Permalloy	/	0.185	1.4×10^6	10.2	55.1	This work
Pure Fe	/	1.1	6×10^6	16.3	14.8	This work
Fe–Si–B	/	0.1	9×10^5	6.6	66	This work
FNMG-5	/	0.1	9.3×10^5	39.7	397	This work

| FNMG-10 | / | 0.1 | 9.8×10^5 | 35.4 | 354 | This work |
| FNMG-15 | / | 0.1 | 10.8×10^5 | 23.5 | 235 | This work |

Reference

(1) Kong, J. A. *Electromagnetic wave Theory, John Wiley & Sons,* 2000.

(2) Sarto, M. S. A matrix surface impedance formulation for the analysis of EM-interactions to finite laminated composite slabs. Electromagnetic Compatibility, 1996. Symposium Record. IEEE 1996 International Symposium on. *IEEE,* **1996**: 168-173.

(3) Sarto, M. S.; Michele, D. S.; Leerkamp, P. Electromagnetic performance of innovative lightweight shields to reduce radiated emissions from PCBs. *IEEE trans. Electromagn. Compat.* **2002**, *44* (2), 353-363.

(4) Al-Saleh, M. H.; Sundararaj, U. Electromagnetic interference shielding mechanisms of CNT/polymer composites. *Carbon* **2009,** *47*, 1738-1746.

(5) Al-Saleh, M. H.; Saadeh, W. H.; Sundararaj, U. EMI shielding effectiveness of carbon based nanostructured polymeric materials: A comparative study. *Carbon* **2013,** *60*, 146-156.

(6) Maiti, S.; Shrivastava, N. K.; Suin, S.; Khatua, B. B. Polystyrene/MWCNT/ graphite nanoplate nanocomposites: efficient electromagnetic interference shielding material through graphite nanoplate-MWCNT-graphite nanoplate networking. *ACS Appl. Mater. Interfaces* **2013,** *5* (11), 4712-24.

(7) Chung, D. D. L. Electromagnetic interference shielding effectiveness of carbon materials. *Carbon* **2001,** *39*, 279-285.